



**HAL**  
open science

## Three-dimensional right-ventricular regional deformation and survival in pulmonary hypertension

Pamela Mocerì, Nicolas Duchateau, Delphine Baudouy, Elie-Dan Schouver, Sylvie Leroy, Fabien Squara, Emile Ferrari, Maxime Sermesant

► **To cite this version:**

Pamela Mocerì, Nicolas Duchateau, Delphine Baudouy, Elie-Dan Schouver, Sylvie Leroy, et al.. Three-dimensional right-ventricular regional deformation and survival in pulmonary hypertension. *European Heart Journal - Cardiovascular Imaging*, 2018, 19, pp.450-458. 10.1093/ehjci/jex163 . hal-01533793

**HAL Id: hal-01533793**

**<https://inria.hal.science/hal-01533793>**

Submitted on 6 Jun 2017

**HAL** is a multi-disciplinary open access archive for the deposit and dissemination of scientific research documents, whether they are published or not. The documents may come from teaching and research institutions in France or abroad, or from public or private research centers.

L'archive ouverte pluridisciplinaire **HAL**, est destinée au dépôt et à la diffusion de documents scientifiques de niveau recherche, publiés ou non, émanant des établissements d'enseignement et de recherche français ou étrangers, des laboratoires publics ou privés.

## **Three-dimensional right-ventricular regional deformation and survival in pulmonary hypertension**

---

Pamela Mocerì \*<sup>a,b,c</sup>; Nicolas Duchateau \*<sup>a</sup>; Delphine Baudouy<sup>b</sup>; Elie-Dan Schouver<sup>b,c</sup>; Sylvie  
Leroy<sup>d</sup>; Fabien Squara<sup>b</sup>; Emile Ferrari<sup>b,c</sup>; Maxime Sermesant<sup>a</sup>.

Short title: 3D RV in pulmonary hypertension

Manuscript total word count: 5299

\* The first 2 authors contributed equally to the manuscript

<sup>a</sup> Université Côte d'Azur, Inria Asclepios team, Sophia Antipolis, France.

<sup>b</sup> Cardiology Department, Hôpital Pasteur, CHU de Nice, Nice, France.

<sup>c</sup> Faculté de médecine, Université Côte d'Azur, Nice, France.

<sup>d</sup> Department of Pneumology, Hôpital Pasteur, CHU de Nice, Nice, France.

Corresponding author: Dr Pamela Mocerì, CHU de Nice – Hôpital Pasteur

Avenue de la voie romaine, CS 51069 – 06001 Nice, France.

Tel: + 33 492037733 / Fax: + 33 492038516

Email: [moceri.p@chu-nice.fr](mailto:moceri.p@chu-nice.fr)

## **ABSTRACT**

**Background:** Survival in pulmonary hypertension (PH) relates to right ventricular (RV) function. However, the RV unique anatomy and structure limit 2D analysis and its regional 3D function has not been studied yet. The aim of this study was to assess the implications of global and regional 3D RV deformation on clinical condition and survival in adults with PH and healthy controls.

**Methods and Results:** We collected a prospective longitudinal cohort of 104 consecutive PH patients and 34 healthy controls between September 2014 and December 2015. Acquired 3D transthoracic RV echocardiographic sequences were analysed by semi-automatic software (TomTec 4D RV-Function 2.0). Output meshes were post-processed to extract regional motion and deformation. Global and regional statistics provided deformation patterns for each subgroup of subjects.

RV lateral and inferior regions showed the highest deformation. In PH patients, RV global and regional motion and deformation (both circumferential, longitudinal and area strain) were affected in all segments ( $p < 0.001$  against healthy controls). Deformation patterns gradually worsened with the clinical condition. Over 6.7 [5.8-7.2] months follow-up, 16 (15.4%) patients died from cardio-pulmonary causes. Right atrial pressure, global RV area strain, TAPSE, 3D RV ejection fraction and end-diastolic volume were independent predictors of survival. Global RV area strain  $> -18\%$  was the most powerful RV function

parameter, identifying patients with a 48%-increased risk of death (AUC 0.83 [0.74-0.90],  $p < 0.001$ ).

**Conclusions:** RV strain patterns gradually worsen in PH patients and provide independent prognostic information in this population.

**KEYWORDS:** pulmonary hypertension; three-dimensional echocardiography; speckle-tracking imaging.

## **ABBREVIATIONS**

AS	Area strain
EDV	End-diastolic volume
EF	Ejection fraction
HR	Hazard ratio
IVA	Myocardial acceleration during isovolumic contraction
LV	Left ventricle
PA	Pulmonary artery
PAH	Pulmonary arterial hypertension
PH	Pulmonary hypertension
RV	Right ventricle
RVOT	Right ventricular outflow tract
SD	Standard deviation
TAPSE	Tricuspid annular plane systolic excursion
VTI	Velocity time integral
WHO	World Health Organization

## **INTRODUCTION**

Pulmonary hypertension (PH) is a severe condition, responsible for symptoms and premature death related to right ventricular (RV) function and remodelling (1-4). In clinical practice, two-dimensional (2D) echocardiography is the most common RV imaging modality, especially in the setting of PH. Transthoracic 2D ultrasound provides a number of descriptors for evaluating right heart haemodynamic but is limited by the anterior position of the tripartite RV and the 2D one-slice plane.

Strain estimation using speckle-tracking on 3D echocardiographic sequences has been suggested as a better means of assessing RV function (5,6), due to the singular anatomy and structure of the RV, and the inherent 3D nature of cardiac deformation. However, little is known about the deterioration of 3D RV function and deformation with disease, and their relation with survival. Descriptors of shape, sphericity (7,8) and curvature (9-11) have been proposed, but overall regional RV strain changes have not been studied yet. RV free wall peak longitudinal strain and transverse strain have previously been shown to relate to cardiovascular events and mortality in pulmonary hypertension (12-17), but finer markers and analyses are required (18,19). We hypothesized that the analysis of regional 3D RV strain spatiotemporal patterns, which has not been performed yet, could provide additional insights into the deterioration of RV function and survival.

To do so, we extracted both global and regional 3D RV deformation, and we adapted efficient computational tools to these new types of RV data. Based on these descriptors, we assessed whether statistical differences exist between patients with PH and healthy controls, and related them with clinical outcome.

## **METHODS**

### ***Study design and patients***

We performed a prospective longitudinal study on PH patients followed up at our centre (Pasteur University Hospital, Nice, FR) between September 2014 and December 2015. Consecutive clinically stable PH patients were enrolled into a standardized echocardiographic protocol. Healthy controls were enrolled to help determining normal values of 3D RV deformation imaging with our software. Our local research Ethics committees approved this study protocol, which conforms to the ethical guidelines of the 1975 Declaration of Helsinki.

Adult PH patients who consented to the study were included. Pre-capillary PH was considered according to right heart catheterization data, when mean pulmonary artery pressure at rest was  $\geq 25$  mmHg with pulmonary capillary wedge pressure  $\leq 15$  mmHg. Patients with significant left heart disease, arrhythmias or poor acoustic windows were excluded. Patients with chronic thromboembolic pulmonary hypertension were excluded if they had been scheduled for either endarterectomy or pulmonary angioplasty. Patients with PH due to lung diseases and/or hypoxemia were included only if they were considered as stable (regarding the respiratory status) for at least 3 months and already under oxygen if needed. Asymptomatic healthy volunteers were recruited from the community to serve as

controls and included if they had a normal trans-thoracic echocardiography, and if they were in sinus rhythm.

Demographics, clinical data (age, gender, diagnosis, baseline WHO class, PH-targeted advanced therapy), BNP plasma levels (Beckman Access 2, Triage BNP assay (Biosite Diagnostics Inc, San Diego, CA)) and 6-minute walk test distance were collected at baseline. The time of echocardiography was considered as the start date for the study enrolment (the ultrasound qualifying the patient for inclusion). Follow-up was considered from the date of echocardiography and continued until patients either died or reached the end of the study (December 2015). Clinical outcome was defined by mortality related to PH.

### ***2D-echocardiographic acquisitions and measurements***

Echocardiographic examination was performed using an IE-33 or EPIQ-7 ultrasound system and a S5 or X5-1 transducer (Philips Medical system, Andover, MA). Doppler echocardiography was performed according to the recommendations of the American Society of Echocardiography (ASE) / European Association for Cardiovascular Imaging (EACVI) (20-22).

Two different staff cardiologists, with advanced training in echocardiography, performed the cine-loops acquisitions and interpreted 2D-echo datasets. The measured parameters were averaged over three consecutive cycles. The following parameters were

measured: left ventricular ejection fraction, right atrial area, tricuspid annular peak systolic velocity (s'), myocardial acceleration during isovolumic contraction (IVA) (23), tricuspid annular plane systolic excursion (TAPSE), systolic pulmonary artery pressure (derived from the tricuspid valve regurgitation), right ventricular outflow tract (RVOT) velocity-time integral (VTI) and right atrial pressure estimated on the basis of IVC diameter and collapse (20).

### ***3D Trans-thoracic Echocardiography***

At least four 3D cine-loops of the RV were acquired from an apical 4-chamber view focused on the RV, using an IE-33 or EPIQ-7 ultrasound system and a matrix-array X5-1 transducer (Philips Medical system, Andover, MA). Full-volume acquisition over 2 heartbeats (for loop storage) was performed using ECG-gating over 4-to-6 cardiac cycles, during a quiet breath-hold. Frame rate was maximized to allow the use of the RV-dedicated quantification software. Care was taken to include the entire RV within the images. Digital 3D data sets were stored and analysed using commercial software dedicated to the RV (4D RV Function 2.0, TomTec Imaging Systems GmbH, DE) (Figure 1). This software allowed tracking the RV endocardium along the cardiac cycle using 3D speckle-tracking. It directly estimated the RV end-diastolic and end-systolic volumes, ejection fraction, and wall-specific

peak strain. Test-retest variability (intra-operator, inter-loop and inter-operator variability) was also assessed in a randomly selected group of 10 patients and 10 healthy controls.

### ***Displacement and deformation analysis***

Motion and deformation were analysed at each point of the RV endocardium and at each instant of the cycle. Motion (3D displacement) was projected along the radial, circumferential and longitudinal directions. Circumferential and longitudinal strains were computed as the *engineering strain* ---the relative change of length--- along these directions, within a 5 mm neighborhood. Area strain was computed as the area change of each mesh triangle. Due to the availability of endocardial surfaces only, radial strain was not computed. We used the mesh correspondences provided by the commercial software to label the RV regions according to *Haddad et al.* (24) (Figure 2).

These computations were done using VTK (v 7.10, Kitware, New York, US), and Matlab (v.R2011a, MathWorks, Natick, US), as previously validated in (25).

### ***Right heart catheterization***

Right heart catheterization was performed on 67 patients within 2 months from the ultrasound examination and in the same day on 29 patients as part of their standard treatment plan and follow-up.

### ***Statistical analysis***

Data were summarized as mean  $\pm$  standard deviation for continuous variables with normal distribution; median [95% confidence interval] for other continuous variables and number of subjects (%) for categorical variables. The variables were tested by the Student t-test for normally distributed variables otherwise, Mann-Whitney U-test was performed. Categorical variables were compared using Fisher's exact test. Bonferroni correction was used for multiple comparisons. Right heart catheterization data were correlated to global area strain using the Pearson test. The relationship between echocardiographic parameters and survival was assessed through univariate and multivariate Cox proportional hazard regression, starting at the date of echocardiography. Multivariate survival analysis included all variables with a p-value  $<0.10$  in the univariate analysis as well as previously described prognostic parameters: WHO functional class, BNP, 6-minute walking distance and PH-targeted advanced therapy. Receiver operating characteristics curves were constructed to derive the optimal cut-off values to predict survival (Youden's index method). Test-retest variability consisted of intra- and inter-operator comparisons as well as inter-loop strain comparisons, and included intra-class correlation coefficients. For all analyses, statistical significance was defined as a p-value  $<0.05$ . Statistical analyses were performed using MedCalc 16.1 (MedCalc Software, Mariakerke, BE).



## **RESULTS**

### ***Baseline characteristics***

One hundred four consecutive adult PH patients and 34 healthy controls were included in the study. One hundred seventeen patients were initially screened, 13 were excluded because of atrial fibrillation in 4 of them and poor acoustic window in the other 9. Table 1 summarizes baseline characteristics for patients and healthy controls.

Our patients' population included 65 (62.5%) group 1 pulmonary arterial hypertension (PAH) patients (detailed below), 26 (25.0%) group 3 PH patients, 11 (10.6%) group 4 PH patients and 2 (1.9%) group 5 PH patients according to the most recent PH classification (26). PAH aetiology was idiopathic PAH in 17 patients (26.2% of group 1 PAH patients), heritable PAH in 1 patient (1.5%), 4 drug- and toxin-induced PAH (6.2%), PAH associated with connective tissue disease in 16 patients (24.6%), associated with congenital heart disease in 13 patients (20%) (including 4 ventricular septal defects, 4 atrial septal defects, 1 complete atrio-ventricular septal defect and 4 closed left-to-right shunts), associated with portal hypertension in 12 (18.5%) patients, and HIV-associated PAH in 2 patients (3.1%). All group 1, 4 and 5 patients as well as 9 patients from group 3 PH were treated with advanced targeted PAH therapy at baseline.

Eighty-six PH patients (82.7%) had a reduced RV ejection fraction <45%, 43 of them (41.3%) had a TAPSE below 20 mm and 52 (50%) a BNP level above 100 ng/mL.

The full 3D RV analysis using TomTec software required an average of  $185 \pm 42$  seconds including image alignment and manual correction of the detected endocardial RV borders.

### ***RV segmental and global strain***

Global and regional RV strain comparisons between patients and healthy controls are summarized in Tables 1 and 2. In healthy controls, area strain predominated at the lateral and inferior wall. Circumferential and longitudinal RV strain predominated at the lateral and inferior wall, respectively. The septal component of the RV also contributed to the global RV deformation. As compared to healthy controls, PH patients had significantly reduced global and regional RV area strain (in all RV segments,  $p < 0.001$ ). Similar observations were made for the RV longitudinal and circumferential strain in all segments.

### ***Link with the severity of the disease***

A gradient in RV area strain was observed according to the severity of the disease (assessed by baseline WHO functional class, Figure 3 and 4). It was accompanied by a gradual dilatation of the RV (Table 3). Apart from this gradual decrease in the peak deformation, a slight but gradual delay in the contraction was also associated with the WHO class, as visible in all the strain components at the segments with higher contraction (RV

lateral, Figure 5). We tested the correlation between global RV area strain and invasive parameters collected the same day in a subset of 29 patients. None of the invasive parameters were significantly associated with global RV area strain: pulmonary vascular resistance ( $r=0.10$ ;  $p=0.4$ ); mean pulmonary artery pressure ( $r=0.20$ ;  $p=0.3$ ); cardiac index ( $r=-0.16$ ;  $p=0.4$ ); right atrial pressure ( $r=-0.12$ ;  $p=0.6$ ). On the opposite, RV ejection fraction was closely associated to RV global area strain ( $r=-0.90$ ,  $p<0.0001$ ).

### ***Survival analysis***

Over a median follow-up of 6.7 months [5.8–7.2], 16 patients (15.4%) died from cardio-pulmonary causes. On univariate survival analysis, baseline WHO functional class IV (HR 2.89 [1.08-7.72];  $p=0.03$ ), 6-minute walking distance (HR 0.98 [0.97-1.00];  $p=0.05$ ), PH-targeted advanced therapy (HR 0.24 [0.09-0.67];  $p=0.006$ ), BNP (HR 1.002 [1.001-1.003];  $p<0.001$ ), invasive mean PA pressure (HR 1.06 [1.01-1.11];  $p=0.02$ ) were predictors of survival. Echocardiographic predictors of survival on univariate analysis included 3D RV ejection fraction (HR 0.87 [0.81-0.93];  $p<0.001$ ), 3D RV end-diastolic volume (HR 1.02 [1.01-1.03];  $p<0.001$ ), moderate or severe tricuspid regurgitation (HR 8.45 [3.08-23.15];  $p<0.001$ ), systolic PA pressure (HR 1.03 [1.01–1.05];  $p=0.009$ ), right atrial pressure (HR 1.41[1.24-1.61];  $p<0.001$ ), right atrial area (HR 1.08 [1.05-1.12];  $p<0.001$ ), pulmonary VTI (HR 0.86 [0.75-0.98];  $p=0.02$ ), tricuspid s' (HR 0.82 [0.69-

0.97];  $p=0.02$ ), TAPSE (HR 0.8 [0.72-0.90];  $p<0.001$ ), global RV area strain (HR 1.34 [1.18-1.52];  $p<0.001$ ), global RV circumferential strain (HR 1.53 [1.24-1.88];  $p<0.001$ ) and global RV longitudinal strain (HR 1.31 [1.10-1.56];  $p=0.002$ ).

On multivariate analysis including baseline WHO functional class, BNP, 6-minute walking distance and PH-targeted advanced therapy as covariates, global area strain (HR 1.72 [1.07-2.78];  $p=0.03$ ), 3D RV ejection fraction (HR 0.80 [0.64-0.99], 3D RV end-diastolic volume (HR 1.03 [1.00-1.05];  $p=0.02$ ), TAPSE (HR 0.72 [0.52-0.99];  $p=0.04$ ) and right atrial pressure (HR 1.61 [1.09-2.36];  $p=0.02$ ) were independent predictors of survival.

On receiver operating curve analysis, the average area under the curve for the global RV area strain was 0.83 [0.74-0.90],  $p<0.001$  compared to 0.81 [0.72-0.88],  $p<0.001$  for TAPSE and 0.80 [0.71-0.87],  $p<0.001$  for 3D RV ejection fraction (Figure 6). Global RV area strain  $> -18\%$  identified patients at high risk of mortality with a sensitivity of 94% and a specificity of 62%.

### ***Reproducibility***

Intra-class correlation coefficients for inter-observer variability were 0.90 [0.77-0.96] for RV EF and 0.94 [0.86-0.98] for RV EDV. Intra-class correlation coefficients for intra-observer variability (same cine loop analysed) were 0.95 [0.88-0.98] for RV EF, 0.98 [0.96-0.99] for RV EDV and 0.93 [0.83-0.97] for RV global area strain, respectively. Intra-class correlation

coefficients for inter-loop variability (intra-observer variability using a second dataset acquired at a different time) were 0.94 [0.86-0.98] for RV EF, 0.94 [0.86-0.98] for RV EDV and 0.94 [0.86-0.98] for RV global area strain.

## **DISCUSSION**

Studying the RV function is challenging but of critical importance, especially in a devastating disease such as pulmonary hypertension. Our study analysed for the first time RV 3D deformation patterns in healthy controls and pulmonary hypertension patients using dedicated RV software. Our results highlight the role of regional deformation analysis, which reveal the dominant RV regions (inferior and lateral wall) and subtle pattern changes with disease severity. This study also demonstrates the prognostic role of RV area strain in PH patients.

### ***2D vs 3D RV analysis and regional function***

Standard evaluation of the RV usually requires 2D assessment (20). Despite being correlated with MRI RV EF, widely used parameters such as TAPSE and TV s' (to assess RV function in routine clinical practice) only assess the lateral tricuspid annulus. 2D speckle-tracking echocardiography has been used to quantify RV myocardial deformation, but mainly focuses on longitudinal strain. Indeed, given the complex anatomy of the RV, circumferential strain cannot be fully assessed by 2D techniques. Actually, MRI studies have highlighted the value of considering RV circumferential strain for some pathologies such as arrhythmogenic RV cardiomyopathy (27) or RV afterload changes (28,29). Besides, going beyond global measurements and assessing regional RV function is determinant in the

evaluation of Tetralogy of Fallot patients (30-32) and pulmonary embolism (33,34), but is usually assessed with MRI. In this study, we demonstrate using dedicated software the feasibility and high value of 3D echocardiographic analysis to estimate RV ejection fraction, volumes (35), and regional RV function (36) in healthy volunteers and PH patients. We also believe that adding circumferential strain to the longitudinal RV strain analysis, which allows computing RV area strain, provides additional prognostic information.

The tracking accuracy and therefore the relevance of motion and deformation values were fully conditioned by the Tomtec commercial software, whose use has been validated in (37). Our post-processing software only uses standard mathematical formulations to compute *local* motion and deformation from already existing mesh data, and corresponds to the validated tools (25).

Our study provides a new statistical characterization of 3D RV deformation patterns. It first illustrates the normal contraction pattern over the whole RV: the lateral wall is predominant in terms of area strain, but the inferior wall, the anterior wall as well as the inlet septum are also significant contributors to the RV global area change. Longitudinal deformation predominates at the inferior wall, whereas the lateral wall provides more circumferential deformation. Then, this statistical characterization is extended to the comparison of PH against healthy deformation patterns, and confirms that RV dysfunction predominates in these regions.

### ***RV remodelling and outcome***

Our method provided a reliable full analysis of the right ventricle, including regional analysis. Using left ventricle-dedicated software, previous studies already reported that RV global area strain is associated with outcomes in PH (16,38,39). Our results confirm the prognostic role of RV area strain. The use of dedicated RV software allowed studying the entire RV structure and refining observations at the regional level. Despite playing a “minor” role as compared to the lateral, anterior and inferior wall, the RVOT and infundibular septum significantly contribute to RV area strain. This opens the door to complementary analyses of the RV function in PAH, such as the timing alteration of RV segments.

RV adverse remodelling, RV dilatation and reduction in RVEF and/or area strain are associated with mortality in our cohort of PH patients. Cardiac index, a known but debated invasive indicator of prognosis reflecting RV contractility (40), did not reach statistical significance in our cohort, probably because of the low number of patients with right heart catheterization data. RV area strain is independently and strongly associated with survival, illustrating the initial role of decreasing strain before reducing RV EF and dilating the cavity. Indeed, our echocardiographic parameter could be interpreted as a consequence of the RV-PA unit, a marker of RV-PA coupling (41), which among other parameters has been

recently related to prognosis in PH (42). Finer markers of RV function like area strain are therefore useful to detect early changes in PAH patients and could help improving the follow-up and prognosis of such patients.

### ***Limitations***

3D RV analysis was feasible in 88.9% of patients, the main limitation being the imaging quality. Given the expected intra-individual variability, patients with atrial fibrillation were excluded from this preliminary study. This could represent a selection bias. Patients with post-capillary PH were not studied and the conclusions made in this paper are consequently not extendable to this population. Indeed, left heart disease could influence RV deformation.

Classically, 3D RV assessment was limited by its feasibility. In our study, thanks to RV dedicated software, intra- and inter-operator and inter-loop reproducibility were acceptable, as previously described (37). Furthermore, the duration of the 3D quantification analysis was acceptable and could be applicable in routine clinical practice.

Our cohort of control patients was relatively small, as compared to the PH group. Indeed, identifying patients in the Echo Lab, without any structural heart disease (potentially influencing RV remodelling) has been very difficult. Furthermore, this issue

prevents us from age-matching our control population to the PH population. Indeed, this could represent another limitation given that age could influence 3D RV quantification (43).

The lack of correlation between haemodynamic parameters and RV area strain can be confusing. However, this could be expected, as the number of patients with invasive data was relatively low compared to the overall number of patients. Right atrial pressure, a strong marker of risk in PH patients was also a predictor of mortality in our population, but not related to RV area strain. This might be explained by the evolution of PH itself as right atrial pressure increases gradually with RV dysfunction, while RV area strain might be an earlier marker of RV dysfunction, explaining the relative independence of both markers.

The prognostic importance of decreased RV area strain is obvious in our cohort, however as our patients suffer from multiple PH aetiologies, a larger multicentre study could help verifying and generalizing our conclusions in a larger population. Given the relatively small cohort of patients, no etiological subgroup analysis was performed. A larger study would allow describing RV shape and deformation patterns in a finer way for each PH aetiology, especially in group 1 patients.

## **CONCLUSIONS**

We examined the implications of a finer analysis of 3D RV deformation on clinical condition and survival in a cohort of adults with PH and 34 healthy controls. We quantitatively demonstrated that RV strain patterns gradually worsen in PH patients and provide independent prognostic information. This new technique could help better stratifying the risk in PH patients.

## **ACKNOWLEDGMENTS**

Funding sources: The software license TomTec 4D RV Function 2.0 (TomTec Imaging Systems GmbH, DE) was funded by the AO2I of the University hospital of Nice, France. This study was partly funded by a grant from the University hospital of Nice, France (AOI-2014). The authors also acknowledge the partial support from the European Union 7th Framework Programme (VP2HF FP7-2013-611823) and the European Research Council (MedYMA ERC-AdG-2011-291080).

**DISCLOSURES:** None.

## **REFERENCES**

1. Galie N, Rubin L, Simonneau G. Developing a heart score: next steps. *Am J Cardiol.* 2012;**110**:49S-51S.
2. Raymond RJ, Hinderliter AL, Willis PW, Ralph D, Caldwell EJ, Williams W, *et al.* Echocardiographic predictors of adverse outcomes in primary pulmonary hypertension. *J Am Coll Cardiol.* 2002;**39**:1214-9.
3. Forfia PR, Fisher MR, Mathai SC, Houston-Harris T, Hemnes AR, Borlaug BA, *et al.* Tricuspid annular displacement predicts survival in pulmonary hypertension. *Am J Respir Crit Care Med.* 2006;**174**:1034-41.
4. Mocerri P, Dimopoulos K, Liodakis E, Germanakis I, Kempny A, Diller GP, *et al.* Echocardiographic predictors of outcome in Eisenmenger syndrome. *Circulation.* 2012;**126**:1461-8.
5. Mocerri P, Baudouy D, Chiche O, Gerboni P, Bouvier P, Chaussade C, *et al.* Imaging in pulmonary hypertension: Focus on the role of echocardiography. *Arch Cardiovasc Dis.* 2014;**107**:261-71.
6. Mertens LL, Friedberg MK. Imaging the right ventricle--current state of the art. *Nat Rev Cardiol.* 2010;**7**:551-63.

7. Douglas PS, Morrow R, Ioli A, Reichek N. Left ventricular shape, afterload and survival in idiopathic dilated cardiomyopathy. *J Am Coll Cardiol*. 1989;**13**:311-5.
8. Tischler MD, Niggel J, Borowski DT, LeWinter MM. Relation between left ventricular shape and exercise capacity in patients with left ventricular dysfunction. *J Am Coll Cardiol*. 1993;**22**:751-7.
9. Reisner SA, Azzam Z, Halmann M, Rinkevich D, Sideman S, Markiewicz W, *et al*. Septal/free wall curvature ratio: a noninvasive index of pulmonary arterial pressure. *J Am Soc Echocardiogr*. 1994;**7**:27-35.
10. Sciancalepore MA, Maffessanti F, Patel AR, Gomberg-Maitland M, Chandra S, Freed BH, *et al*. Three-dimensional analysis of interventricular septal curvature from cardiac magnetic resonance images for the evaluation of patients with pulmonary hypertension. *Int J Cardiovasc Imaging*. 2012;**28**:1073-85.
11. Addetia K, Maffessanti F, Yamat M, Weinert L, Narang A, Freed BH, *et al*. Three-dimensional echocardiography-based analysis of right ventricular shape in pulmonary arterial hypertension. *Eur Heart J Cardiovasc Imaging*. 2015;**17**:564-75.
12. Pirat B, McCulloch ML, Zoghbi WA. Evaluation of global and regional right ventricular systolic function in patients with pulmonary hypertension using a novel speckle tracking method. *Am J Cardiol*. 2006;**98**:699-704.

13. Hardegree EL, Sachdev A, Villarraga HR, Frantz RP, McGoon MD, Kushwaha SS, *et al.* Role of serial quantitative assessment of right ventricular function by strain in pulmonary arterial hypertension. *Am J Cardiol.* 2013;**111**:143-8.
14. Motoji Y, Tanaka H, Fukuda Y, Ryo K, Emoto N, Kawai H, *et al.* Efficacy of right ventricular free-wall longitudinal speckle-tracking strain for predicting long-term outcome in patients with pulmonary hypertension. *Circ J.* 2013;**77**:756-63.
15. Fine NM, Chen L, Bastiansen PM, Frantz RP, Pellikka PA, Oh JK, *et al.* Outcome prediction by quantitative right ventricular function assessment in 575 subjects evaluated for pulmonary hypertension. *Circ Cardiovasc Imaging.* 2013;**6**:711-21.
16. Smith BC, Dobson G, Dawson D, Charalampopoulos A, Grapsa J, Nihoyannopoulos P. Three-dimensional speckle tracking of the right ventricle: toward optimal quantification of right ventricular dysfunction in pulmonary hypertension. *J Am Coll Cardiol.* 2014;**64**:41-51.
17. Mocerì P, Bouvier P, Baudouy D, Dimopoulos K, Cerboni P, Wort SJ, *et al.* Cardiac remodelling amongst adults with various aetiologies of pulmonary arterial hypertension including Eisenmenger syndrome-implications on survival and the role of right ventricular transverse strain. *Eur Heart J Cardiovasc Imaging*; doi 10.1093/ehjci/jew277

18. Reichek N. Right ventricular strain in pulmonary hypertension: flavor du jour or enduring prognostic index? *Circ Cardiovasc Imaging*. 2013;**6**:609-11.
19. Abidov A, Rischard F. Quantitative right ventricular function in pulmonary arterial hypertension: a quest for a more reliable metric. *Echocardiography*. 2016;**33**:174-6.
20. Rudski LG, Lai WW, Afilalo J, Hua L, Handschumacher MD, Chandrasekaran K, *et al*. Guidelines for the echocardiographic assessment of the right heart in adults: a report from the American Society of Echocardiography. *J Am Soc Echocardiogr*. 2010;**23**:685-713.
21. Douglas PS, DeCara JM, Devereux RB, Duckworth S, Gardin JM, Jaber WA, *et al*. Echocardiographic imaging in clinical trials: American Society of Echocardiography standards for echocardiography core laboratories. *J Am Soc Echocardiogr*. 2009;**22**:755-65.
22. Lang RM, Badano LP, Mor-Avi V, Afilalo J, Armstrong A, Ernande L, *et al*. Recommendations for cardiac chamber quantification by echocardiography in adults: an update from the American Society of Echocardiography and the European Association of Cardiovascular Imaging. *Eur Heart J Cardiovasc Imaging*. 2015;**16**:233-70.

23. Ernande L, Cottin V, Leroux PY, Girerd N, Huez S, Mulliez A, *et al.* Right isovolumic contraction velocity predicts survival in pulmonary hypertension. *J Am Soc Echocardiogr.* 2013;**26**:297-306.24.
24. Haddad F, Hunt SA, Rosenthal DN, Murphy DJ. Right ventricular function in cardiovascular disease, part I: Anatomy, physiology, aging, and functional assessment of the right ventricle. *Circulation.* 2008;**117**:1436-48.
25. Duchateau N, De Craene M, Allain P, Saloux E, Sermesant M. Infarct localization from myocardial deformation: Prediction and uncertainty quantification by regression from a low-dimensional space. *IEEE Trans Med Imaging.* 2016;**35**:2340-52.
26. Galiè N, Humbert M, Vachiery JL, Gibbs S, Lang I, Torbicki A, *et al.* 2015 ESC/ERS Guidelines for the diagnosis and treatment of pulmonary hypertension: The Joint Task Force for the Diagnosis and Treatment of Pulmonary Hypertension of the European Society of Cardiology (ESC) and the European Respiratory Society (ERS): Endorsed by: Association for European Paediatric and Congenital Cardiology (AEPC), International Society for Heart and Lung Transplantation (ISHLT). *Eur Heart J.* 2016;**37**:67-119.
27. Prati G, Vitrella G, Allocca G, Muser D, Buttignoni SC, Piccoli G, *et al.* Right ventricular strain and dyssynchrony assessment in arrhythmogenic right ventricular

- cardiomyopathy: cardiac magnetic resonance feature-tracking study. *Circ Cardiovasc Imaging*. 2015;**8**:e003647.
28. Cho EJ, Jiamsripong P, Calleja AM, Alharthi MS, McMahon EM, Khandheria BK, *et al*. Right ventricular free wall circumferential strain reflects graded elevation in acute right ventricular afterload. *Am J Physiol Heart Circ Physiol*. 2009;**296**:H413-20.
29. Pettersen E, Helle-Valle T, Edvardsen T, Lindberg H, Smith HJ, Smevik B, *et al*. Contraction pattern of the systemic right ventricle. *J Am Coll Cardiol*. 2007;**49**:2450-6.
30. Bove T, Vandekerckhove K, Devos D, Panzer J, De Groote K, De Wilde H, *et al*. Functional analysis of the anatomical right ventricular components: should assessment of right ventricular function after repair of tetralogy of Fallot be refined? *Eur J Cardiothorac Surg*. 2014;**45**:e6-12.
31. Wald RM, Haber I, Wald R, Valente AM, Powell AJ, Geva T. Effects of regional dysfunction and late gadolinium enhancement on global right ventricular function and exercise capacity in patients with repaired tetralogy of Fallot. *Circulation*. 2009;**119**:1370-7.
32. Kutty S, Zhou J, Gauvreau K, Trincado C, Powell AJ, Geva T. Regional dysfunction of the right ventricular outflow tract reduces the accuracy of Doppler tissue imaging

- assessment of global right ventricular systolic function in patients with repaired tetralogy of Fallot. *J Am Soc Echocardiogr*. 2011;**24**:637-43.
33. Mediratta A, Addetia K, Medvedofsky D, Gomberg-Maitland M, Mor-Avi V, Lang RM. Echocardiographic diagnosis of acute pulmonary embolism in patients with McConnell's sign. *Echocardiography*. 2016;**33**:696-702.
34. Platz E, Hassanein AH, Shah A, Goldhaber SZ, Solomon SD. Regional right ventricular strain pattern in patients with acute pulmonary embolism. *Echocardiography*. 2012;**29**:464-70.
35. Medvedofsky D, Addetia K, Patel AR, Sedlmeier A, Baumann R, Mor-Avi V, *et al*. Novel approach to three-dimensional echocardiographic quantification of right ventricular volumes and function from focused views. *J Am Soc Echocardiogr*. 2015;**28**:1222-31.
36. Calcuttea A, Chung R, Lindqvist P, Hodson M, Henein MY. Differential right ventricular regional function and the effect of pulmonary hypertension: three-dimensional echo study. *Heart*. 2011;**97**:1004-11.
37. Muraru D, Spadotto V, Cecchetto A, Romeo G, Aruta P, Ermacora D, *et al*. New speckle-tracking algorithm for right ventricular volume analysis from three-dimensional echocardiographic data sets: validation with cardiac magnetic resonance

- and comparison with the previous analysis tool. *Eur Heart J Cardiovasc Imaging*. 2016;**17**:1279-89.
38. Vitarelli A, Mangieri E, Terzano C, Gaudio C, Salsano F, Rosato E, *et al*. Three-dimensional echocardiography and 2D-3D speckle-tracking imaging in chronic pulmonary hypertension: diagnostic accuracy in detecting hemodynamic signs of right ventricular (RV) failure. *J Am Heart Assoc*. 2015;**4**:e001584.
39. Ryo K, Goda A, Onishi T, Delgado-Montero A, Tayal B, Champion HC, *et al*. Characterization of right ventricular remodeling in pulmonary hypertension associated with patient outcomes by 3-dimensional wall motion tracking echocardiography. *Circ Cardiovasc Imaging*. 2015;**8**:e003176.
40. Sitbon O, Benza RL, Badesch DB, Barst RJ, Elliott CG, Gressin V, *et al*. Validation of two predictive models for survival in pulmonary arterial hypertension. *Eur Respir J*. 2015;**46**:152-64.
41. Guihaire J, Haddad F, Boulate D, Decante B, Denault AY, Wu J, *et al*. Non-invasive indices of right ventricular function are markers of ventricular-arterial coupling rather than ventricular contractility: insights from a porcine model of chronic pressure overload. *Eur Heart J Cardiovasc Imaging*. 2013;**14**:1140-9.

42. Vanderpool RR, Pinsky MR, Naeije R, Deible C, Kosaraju V, Bunner C, *et al.* RV-pulmonary arterial coupling predicts outcome in patients referred for pulmonary hypertension. *Heart*. 2015;**101**:37-43.
43. Maffessanti F, Muraru D, Esposito R, Gripari P, Ermacora D, Santoro C, *et al.* Age-, body size-, and sex-specific reference values for right ventricular volumes and ejection fraction by three-dimensional echocardiography: a multicenter echocardiographic study in 507 healthy volunteers. *Circ Cardiovasc Imaging* 2013;**6**:700-10.

## **FIGURE LEGENDS**

**Figure 1:** Example of RV 3D analysis using TomTec 4D RV function 4.0

- A. Initial alignment of 3D dataset and identification of landmarks.
- B. End-systolic verification and editing of endocardial RV borders.

**Figure 2:** RV regions used in our study, according to *Haddad et al.* (24)

**Figure 3:** End-systolic strain patterns according to baseline WHO class: the median pattern over each WHO subgroup is represented on the subgroup average shape.

**Figure 4:** End-systolic global area strain according to baseline WHO class.

**Figure 5:** Motion and deformation along the cycle according to the functional capacity (median and first/third quartiles over each subgroup, at the RV lateral segment).

**Figure 6:** Kaplan-Meier and ROC curves for prediction of survival.

## **TABLES**

**Table 1:** Baseline characteristics of the population, including three-dimensional and RV deformation data.

	<b>Pulmonary hypertension n = 104</b>	<b>Healthy controls n = 34</b>	<b>p-value</b>
<b>Age, y</b>	65.9 [62.0-68.8]	45.5 [33.7-50.4]	<0.001
<b>Female sex, n (%)</b>	58 (55.8%)	15 (44.1%)	0.3
<b>Body surface area, m<sup>2</sup></b>	1.72 ± 0.2	1.75 ± 0.1	0.3
<b>WHO functional class ≥ III</b>	66 (63.4%)		
<b>BNP, ng/mL</b>	126 [94.0-182.0]		
<b>6MWD, m</b>	359.5 ± 106		
<b>AT at baseline, n (%)</b>	87 (83.7%)		
<b>Death, n (%)</b>	16 (15.4%)		
<b>2D Echocardiographic data</b>			
<b>LVEF, %</b>	69.1 ± 8.5		
<b>Right atrial pressure, mmHg</b>	10.0 [10.0-10.0]		
<b>Right atrial surface, cm<sup>2</sup></b>	24.0 [22.4-25.0]		
<b>Pulmonary VTI, cm</b>	15.0 ± 4.7		
<b>Systolic PAP, mmHg</b>	75.2 ± 24.9		
<b>TAPSE, mm</b>	20.4 ± 5.2		
<b>Tricuspid s', cm/s</b>	11.6 ± 3.0		
<b>IVA, m/s<sup>2</sup></b>	2.0 [1.9-2.2]		
<b>RHC data</b>			
<b>PVR, Wood U</b>	6.6[5.9-7.6]		
<b>Mean PAP, mmHg</b>	43.3 ± 12.6 Min-max [25-70]		
<b>Right atrial pressure, mmHg</b>	9.0 [7.0-10.0]		
<b>Cardiac index, L/mn/m<sup>2</sup></b>	2.7 [2.4-2.8]		
<b>3D Echocardiographic data</b>			
<b>RV EF, %</b>	35.6 ± 9.7	55.9 ± 5.8	<0.001
<b>RV EDV, mL</b>	91.0 ± 40.6	51.4 ± 21.9	<0.001

<b>Global Area strain, %</b>	-18.8 ± 5.4	-29.5 ± 4.4	<0.001
<b>Global Circumferential strain, %</b>	-11.6 ± 3.6	-17.3 ± 3.2	<0.001
<b>Global Longitudinal strain, %</b>	-8.4 ± 3.6	-14.1 ± 3.6	<0.001
<b>Frame rate, Hz</b>	17.7 [16.6-18.7]	18.0 [17-19]	0.1

6MWD, 6-minute walk test distance; AT, advanced therapy; BNP, brain natriuretic peptide; EDV, end-diastolic volume; EF, ejection fraction; IVA, myocardial acceleration during isovolumic contraction; LVEF, left ventricular ejection fraction; PAP, pulmonary artery pressure; PVR, pulmonary vascular resistance; RHC, right heart catheterization; RV, right ventricular; TAPSE, tricuspid annular plane systolic excursion; VTI, velocity-time integral.

**Table 2:** RV regional deformation data in healthy and PH subjects.

	<b>Pulmonary hypertension n = 104</b>	<b>Healthy Controls n = 34</b>	<b>p value</b>
<b>Area strain, %</b>			
Anterior wall	-17.8±7.0	-29.5±6.6	<0.001
Inferior wall	-24.4±8.8	-37.9±7.4	<0.001
Lateral wall	-28.5±9.1	-43.4±6.6	<0.001
RVOT anterior	-14.7±6.0	-22.2±5.9	<0.001
Infundibular septum	-17.8±7.0	-27.2±7.1	<0.001
Membranous septum	-14.7±7.6	-23.3±8.1	<0.001
Inlet septum	-16.7±8.2	-27.8±9.4	<0.001
Trabeculated septum	-15.9±6.3	-24.8±7.1	<0.001
<b>Circumferential strain, %</b>			
Anterior wall	-12.9±6.2	-20.8±7.4	<0.001
Inferior wall	-13.4±6.3	-20.4±6.0	<0.001
Lateral wall	-19.0±6.2	-29.5±6.2	<0.001
RVOT anterior	-7.8±3.7	-11.6±4.6	<0.001
Infundibular septum	-12.1±3.8	-16.7±3.9	<0.001
Membranous septum	-8.4±4.0	-11.7±3.5	<0.001
Inlet septum	-10.3±6.1	-14.6±6.5	0.001
Trabeculated septum	-8.7±4.4	-13.1±4.7	<0.001
<b>Longitudinal strain, %</b>			
Anterior wall	-6.5±3.6	-10.8±4.3	<0.001
Inferior wall	-12.2±4.9	-20.3±5.8	<0.001
Lateral wall	-10.5±4.6	-16.0±3.8	<0.001
RVOT anterior	-8.3±5.1	-12.5±5.9	<0.001
Infundibular septum	-7.1±6.1	-11.2±5.8	0.001
Membranous septum	-7.3±6.0	-13.2±6.7	<0.001
Inlet septum	-7.4±5.6	-14.9±7.3	<0.001
Trabeculated septum	-7.8±3.8	-13.4±5.0	<0.001

RV, right ventricular; RVOT, right ventricular outflow tract.

**Table 3:** Three-dimensional and RV deformation data according to baseline WHO functional class in PH patients.

	WHO II n = 38	WHO III n = 46	WHO IV n = 20	p-value II vs III	p-value II vs IV	p-value III vs IV
RV EF, %	38.9 ± 8.7	35.5 ± 8.8	29.4 ± 10.9	0.27	< 0.001	0.04
RV EDV, mL	78.1 ± 29.6	90.6 ± 43.0	116.6 ± 42.7	0.43	0.001	0.04
Global Area strain, %	-20.4 ± 5.4	-18.9 ± 4.4	-15.6 ± 6.1	0.61	0.003	0.05
Global Circumferential strain, %	-12.5 ± 3.4	-11.5 ± 3.2	-10.0 ± 4.3	0.5	0.04	0.4
Global Longitudinal strain, %	-9.3 ± 3.9	-8.6 ± 3.0	-6.3 ± 3.3	0.99	0.007	0.05

EDV, end-diastolic volume; EF, ejection fraction; PH, pulmonary hypertension; RV, right ventricular.

**Three-dimensional right-ventricular regional deformation and survival in  
pulmonary hypertension**

---

**WORD COUNT**

**Abstract** : 237 words

**Manuscript word count** (excluding title page and abstract) : 5299 words

**Number of references** : 43

**Number of figures** : 6

**Number of tables** : 3

Figure 1

Preprint version accepted to appear in European Heart Journal Cardiovascular Imaging.  
Final version of this paper available at <https://academic.oup.com/ehjcm>

[Click here to download Figure Figure 1 EHJCVI.tiff](#)

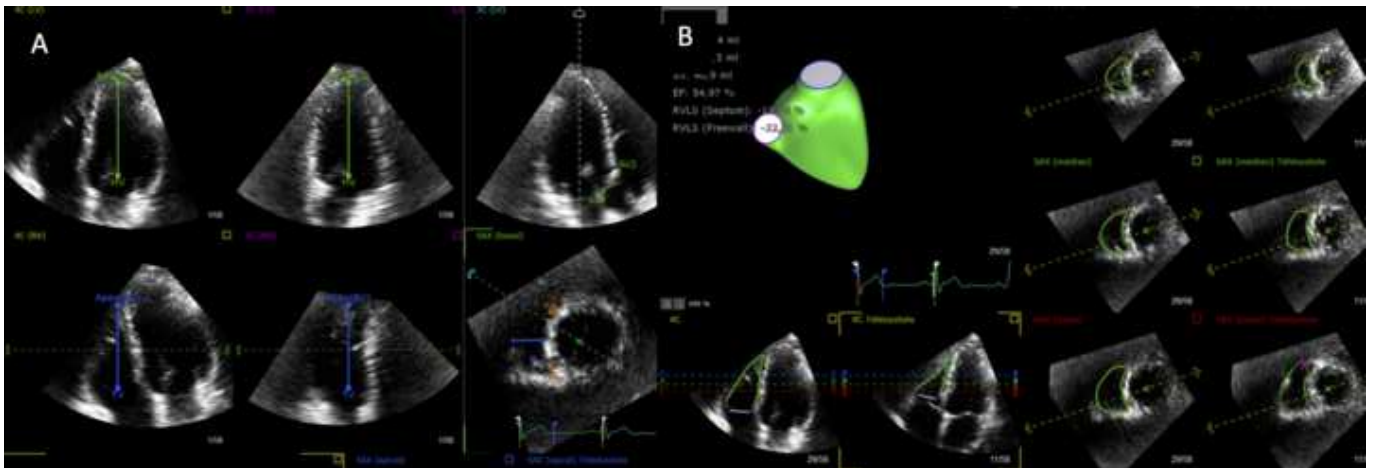


Figure 2

[Click here to download Figure Figure 2 EHJCVI.tiff](#)

Preprint version accepted to appear in European Heart Journal Cardiovascular Imaging.  
Final version of this paper available at <https://academic.oup.com/ehjcm>

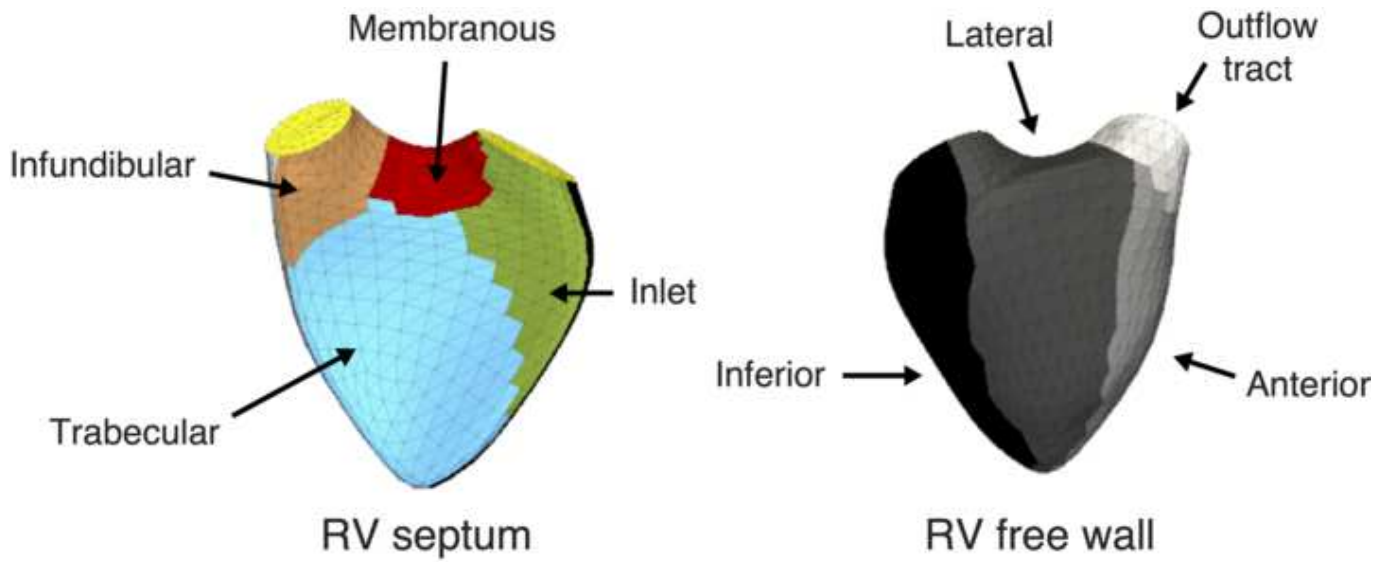


Figure 3

[Click here to download Figure Figure 3.tif](#)

Preprint version accepted to appear in European Heart Journal Cardiovascular Imaging.  
Final version of this paper available at <https://academic.oup.com/ehjcm>

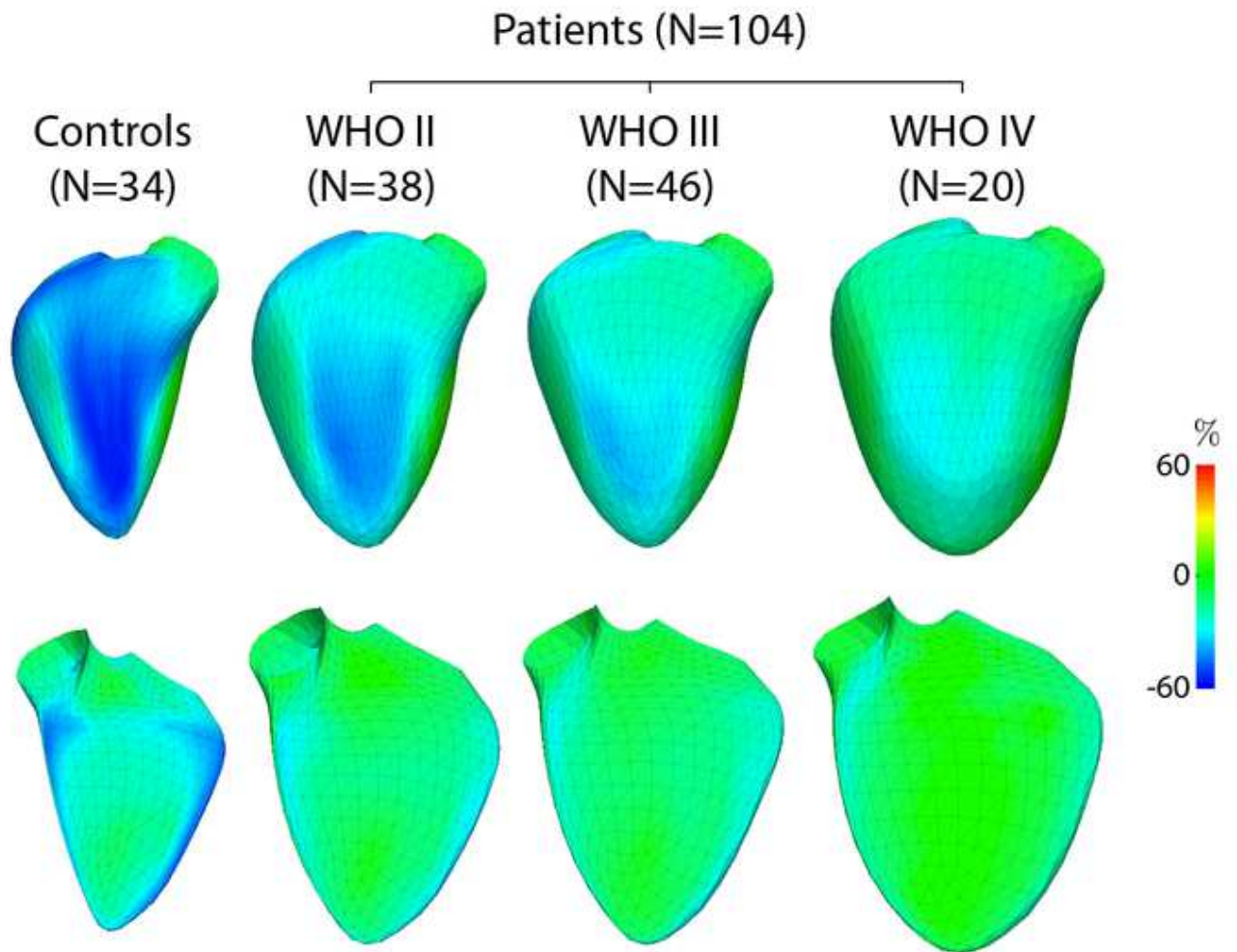


Figure 4

[Click here to download Figure Figure 4 EHCVI.tif](#)

Preprint version accepted to appear in European Heart Journal Cardiovascular Imaging.  
Final version of this paper available at <https://academic.oup.com/ehjcm>

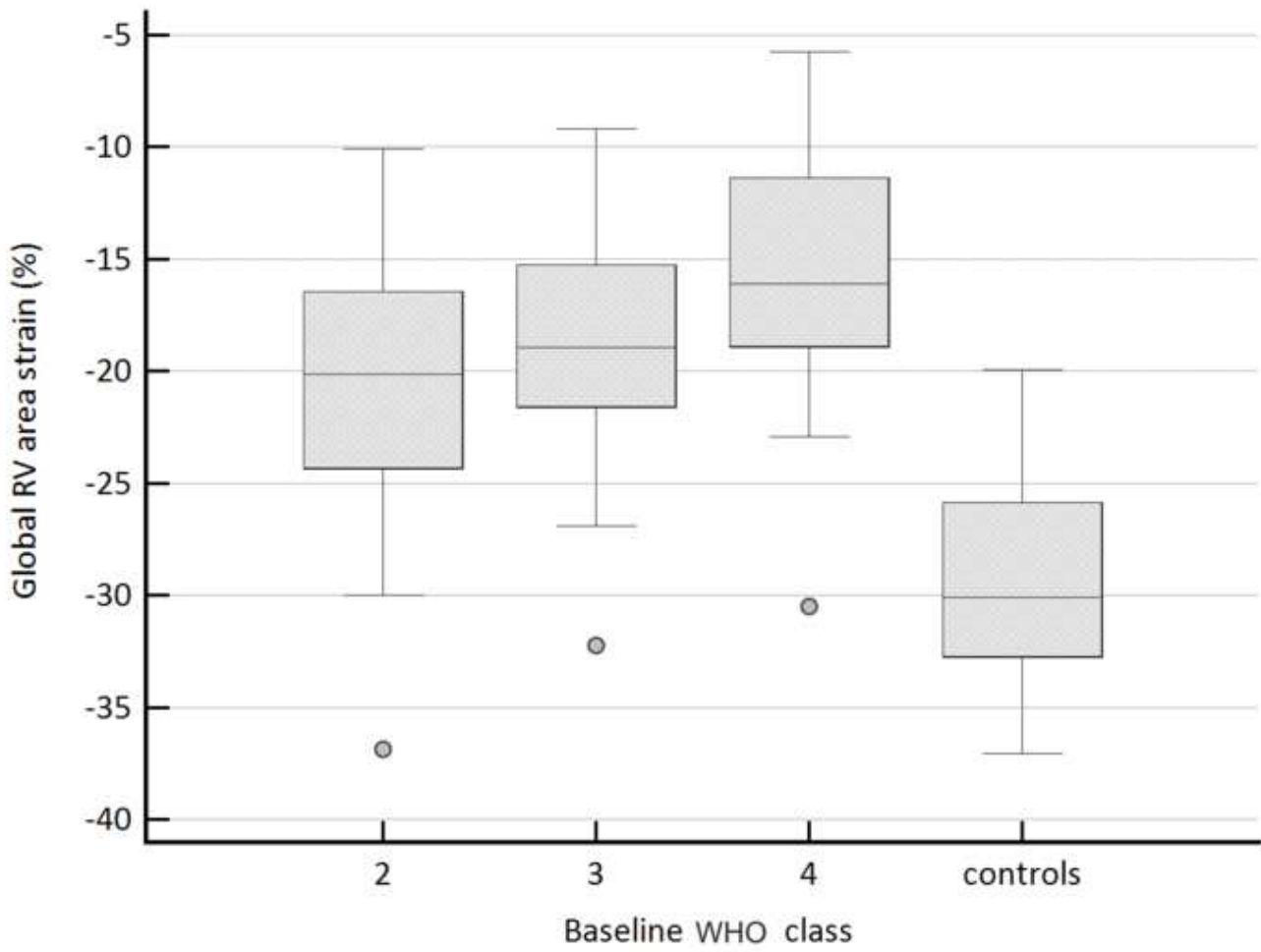


Figure 5

Preprint version accepted to appear in European Heart Journal Cardiovascular Imaging.  
Final version of this paper available at <https://academic.oup.com/ehjcm>

[Click here to download Figure Figure 5.tif](#)

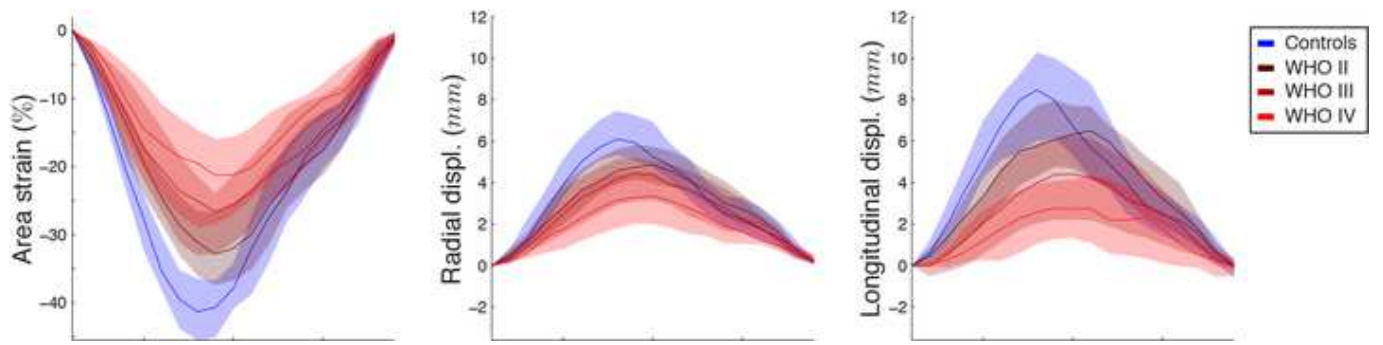


Figure 6

Preprint version accepted to appear in European Heart Journal Cardiovascular Imaging.  
Final version of this paper available at <https://academic.oup.com/ehjcm>

[Click here to download Figure Figure 6.tif](#)

